ACS APPLIED MATERIALS & INTERFACES

RESEARCH ARTICLE

www.acsami.org

Conformal Polymeric Thin Films by Low-Temperature Rapid Initiated Chemical Vapor Deposition (iCVD) Using *tert*-Butyl Peroxybenzoate as an Initiator

Jingjing Xu and Karen K. Gleason*

Department of Chemical Engineering, Massachusetts Institute of Technology, 77 Massachusetts Avenue, Cambridge, Massachusetts 02139, United States

ABSTRACT: Conformal poly(cyclohexyl methacrylate) (pCHMA) thin films were synthesized via initiated chemical vapor deposition (iCVD), with *tert*-butyl peroxybenzoate (TBPOB) as the initiator, representing the first time that TBPOB has been used as an initiator for iCVD synthesis. Using TBPOB instead of *tert*-butyl peroxide (TBPO), the rate of iCVD film growth increased by a factor of up to seven at comparable conformality and lower the filament temperature from 257 to 170 °C at a comparable deposition rate of 3 nm/min. The conformal deposition of functional thin films is desired for applications including microfluidics, medical devices and membranes. Lower filament temperatures reduce the heat load to the deposition surface and thus are advantageous for polymeric substrates that are temperature sensitive or monomers that decompose at high temperatures. Fourier transform infrared spectroscopy (FTIR) and X-ray photoelectron spectroscopy (XPS) results demonstrate the similarity of the TBPOB- to the TBPO-initiated pCHMA main chains. However, the aromatic group in TBPOB provided a unique spectral signature of the polymer chain end group in the FTIR and the peak intensity increased with increase of filament temperature. Scanning electron micrographs (SEMs) revealed that the pCHMA coatings are conformal over non-planar structures; however, at identical process conditions, TBPO-initiated films showed a slightly better conformality due to the lower sticking coefficient of TBPO. At a monomer partial pressure of 0.45, TBPOB has a sticking coefficient value of 0.1188 ± 0.0092, which is ~3 times as high as that of TBPO (0.0413 ± 0.0058). The step coverage is insensitive to filament temperature if the surface concentration of the monomer is fixed.

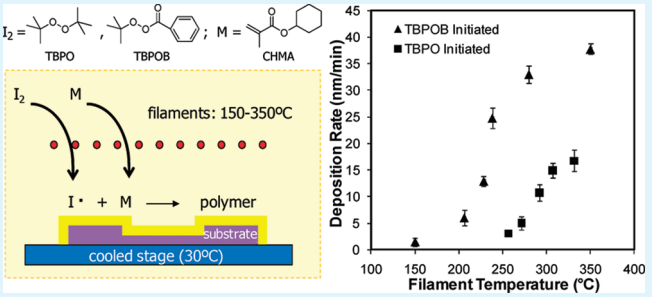

KEYWORDS: chemical vapor deposition, *tert*-butyl peroxybenzoate (TBPOB) initiator, thin films, conformal

INTRODUCTION

Conformal films over nonplanar or porous substrates have attracted increasing interest for applications including microelectromechanical systems (MEMS), medical devices, membranes, and electronic packaging.[1−4] A variety of vapor phase surface modification techniques enable the deposition of thin films with good conformality,[5−7] which is difficult to achieve with solution polymerization techniques because of the surface tension effects. Polymers are a desirable class of materials because of their low cost, ease in fabrication, and wide array of chemical and physical functionalities. Their organic functional groups can be utilized to tune surface energy, to enable subsequent chemical attachment of desirable molecules, or to covalently bind micro- or nanoparticles to the surface.[8,9] Initiated chemical vapor deposition (iCVD) is a polymer chemical vapor deposition technique that utilizes the delivery of vapor-phase monomers to form chemically well-defined polymer films with tunable conformality and properties. Using this technology, a number of functional and biocompatible polymer films have been synthesized and used for applications in microfluidic devices, sensors, and membranes.[10−12] The iCVD method is chemically analogous to solution phase polymerization, but possesses a number of practical advantages. It is able to deposit conformal and pinhole-free coatings on non-planar substrates with nanometer level thickness control.[13−15] In addition, elimination of solvent usage makes the iCVD method compatible with a wide range of substrate materials which swell or dissolve in solution. Furthermore, as a low-energy vapor deposition process, the iCVD process is able to maintain the functionalities from the monomers, which is crucial for subsequent functionalization.[6,16]

A variety of initiator systems can be used to bring about the polymerization. Radicals can be produced by thermal, photochemical, and redox methods.[17] The thermal, homolytic dissociation of initiators is the most widely used mode of generating radicals to initiate polymerization. There are two methods which use thermal initiators with vapor phase monomers. One is to apply non-volatile initiators to the surface and then expose the treated surface to monomer vapors known as vapor-phase assisted surface polymerization (VASP).[18] In order to be introduced into the vacuum chamber as a vapor, the initiator for iCVD must exhibit reasonable volatility. The initiation of chains occurs continuously throughout the iCVD process allowing films of

Received: March 14, 2011
Accepted: June 6, 2011
Published: June 06, 2011

dx.doi.org/10.1021/am200322k | *ACS Appl. Mater. Interfaces* 2011, 3, 2410–2416

arbitrary thickness to be achieved.[19] Additionally the substrate need not be heated to cause the initiator to decompose. To date, iCVD polymerization has utilized primarily thermal initiators including *tert*-butyl peroxide (TBPO),[20−22] *tert*-amyl peroxide,[23] perfluorooctane sulfonyl fluoride,[24] and triethylamine.[25] These molecules contain labile bonds that allow for decomposition of the initiator with a minimal energy input. Indeed, the required filament temperatures are in the range of only ∼200−300 °C for the TBPO initiator. Hence, the initiators can selectively form free radicals at conditions under which the monomeric species are stable allowing complete functional group retention in the deposited polymer chains. Additionally, photoinitiators, such as 2,2′-azobis(2-methylpropane)[26] and benzophenone,[27] can also be used to initiate CVD polymerization by UV irradiation.

Although the reactions of benzoyl peroxide have been studied in great detail by various researchers during the past decades,[28−30] its low vapor pressure makes it difficult to deliver into the vacuum chamber. To use *tert*-butyl peroxybenzoate (TBPOB) as an initiator for iCVD system is challenging because its vapor pressure is only 0.00337 Torr at room temperature, which is much lower than TBPO (27.3 Torr at 25 °C). TBPOB cannot be heated to achieve a higher flow rate because it becomes dangerous during the decomposition reaction under high temperature.[31] The self-accelerating decomposition temperature (SADT) is approximately 65.8 °C. In this work, a bubbler is used to deliver the TBPOB with nitrogen as the patch flow.

TBPOB, a peroxyester, is a strong free radical source. It is used as a polymerization initiator, catalyst and vulcanizing agent, crosslinking agent, and a chemical intermediate.[31] It is much less volatile than TBPO and may enable a higher surface concentration of benzoate radicals and hence has a higher probability to react with the monomer and results in a faster growth rate. TBPOB contains the same weak peroxy (O−O) bond as the TBPO molecule. The TBPO initiated chains will have end groups derived from the t-butoxy radical. Althouh t-butoxy dervived end groups will also be present in the TBPOB initiated films, additionally there will be end groups derived from the oxybenzoate radical. The aromatic group in TBPOB provides a unique spectral signature in the FTIR and may allow quantification of the formation of end groups from the oxybenzoate. Furthermore, with a decomposition temperature of 90 °C in solution, TBPOB holds the potential for further reducing the filament temperature of the iCVD process. Lower filament temperatures are desired for use with polymeric substrates which decompose at high temperature or have low glass transition temperature. Lower filament temperatures are also desired for monomers that decompose at high temperature. In this work, TBPOB has been tested in the iCVD system for the first time and used as an initiator to deposit conformal poly(cyclohexyl methacrylate) (pCHMA) thin films on non-planar substrates, representing the first time that TBPOB has been used as an initiator for iCVD system. The deposition kinetics, films composition and structure, sticking coefficient, and conformality will be compared to iCVD pCHMA films initiated by TBPO.

EXPERIMENTAL SECTION

Deposition Setup. Experiments were performed in a custom built vacuum reactor (Sharon Vacuum) with a radius of 12 cm, as previously described.[14] The ChromAlloy filaments (Goodfellow) were mounted in a parallel array to provide the thermal excitation, heated by a DC power supply (Sorensen). The filament temperature was measured by a K type thermocouple (Omega Engineering) attached to one of the filaments. The vertical distance between the filament and the deposition stage was 1.5 cm. The stage was back-cooled by a recirculating chiller/heater (NESLAB), which served as the purpose of maintaining the substrate temperature constant to prevent the heating of the sample due to the heated filaments. The substrate temperature was set to 30 °C for all the depositions.

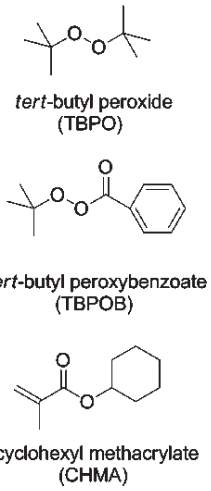

Figure 1. Initiators and monomer used in this work.

tert-Butyl peroxybenzoate was delivered into the reactor at 0.6 sccm via a stainless steel bubbler (Strem Chemicals, Inc.), with nitrogen as the gas carrier. All the chemicals were used as purchased without further purification and their structures are shown in Figure 1. *tert*-Butyl peroxide (Aldrich, 97%) initiator at room temperature was fed into the reactor through a mass flow controller (model 1479, MKS Instruments) at 0.6 sccm. Cyclohexyl methacrylate (CHMA) (Aldrich, 95%) monomer, heated to 80 °C in a glass jar, was delivered into the reactor at 4.6 sccm via a needle valve. The flow rate of nitrogen patch flow was set to 1 sccm for both TBPO and TBPOB initiated depositions. Total pressure in the vacuum chamber was maintained at 0.17 Torr.

Film Characterization. The deposition process was monitored in situ by interferometry with a 633 nm He−Ne laser (JDS Uniphase). Measurements of the film thickness on flat Si wafer substrates were performed on a variable-angle spectroscopic ellipsometry (VASE) (J. A. Woollam M-2000). Samples were measured at an incidence angle of 70° and with a wavelength range of 315−700 nm. In the conformality analysis, film thickness on trench wafers was measured from the SEM cross-sectional images.

Fourier transform infrared (FTIR) measurements were performed on a Nicolet Nexus 870 ESP spectrometer in a normal transmission mode. A deuterated triglycine sulfate (DTGS) KBr detector over the range of 400-4000 cm^{-1} was utilized with a 4 cm^{-1} resolution. Films deposited on Si wafers were measured immediately after deposition, and measurements were averaged over 64 scans to improve the signal-to-noise ratio. All spectra were baseline-corrected by subtracting a background spectrum of the Si wafer substrate. The intensity of the FTIR spectra for films deposited at different filament temperatures was normalized using the peak at 1714.6 cm^{-1} (C═O stretching) as the reference point.

An X-ray photoelectron spectroscopy (XPS) survey spectrum was obtained on a Kratos Axis Ultra spectrometer with a monochromatized Al Kα source, operated at 150 Watts. The pass energy and step size for survey scans was 160 eV and 1 eV. For high-resolution scans, the pass energy and step size was 20 eV and 100 meV. Pressure during analysis was kept under 2×10^{-8} Torr. The analysis area was 400 × 750 μm and the take-off angle for analysis on the Kratos Axis Ultra was 90 degrees. CasaXPS was used to fit the high-resolution spectra, with Shirley as the

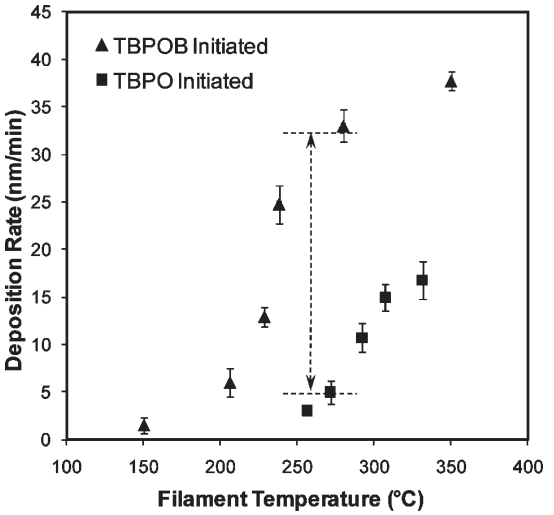

Figure 2. Deposition rate as a function of filament temperature, with TBPOB and TBPO as initiators. Flow rates of CHMA monomer, TBPO, and TBPOB initiators are 4.6, 0.6, and 0.6 sccm. The substrate temperature is 30 °C and monomer partial pressure ratio is 0.45 for both sets of experiments.

background. The FWHM constraints were set at (0, 1.2). Relative sensitivity factors were calibrated by measuring a standard poly(cyclohexyl methacrylate) polymer (Aldrich) spun-cast onto a Si wafer. TBPO-, TBPOB-initiated, and standard pCHMA samples were stored under vacuum overnight prior to analysis.

Both TBPO- and TBPOB-initiated pCHMA films were deposited on silicon substrates patterned with trenches supplied by Analog Devices. These trenches were 7 μm deep and 0.8, 1.3, 2.1, and 5 μm wide, respectively. Deposited trench wafers were sputter-coated with 6 nm of gold (Denton Desk II), and SEM images were obtained by a JEOL JSM-6060 with acceleration voltage of 5 kV.

RESULTS AND DISCUSSION

Deposition Kinetics. Figure 2 shows the deposition rate as a function of filament temperature using TBPO and TBPOB as initiators for iCVD pCHMA, respectively. The deposition rate increases as the filament temperature increases for both initiators. As the filament temperature increases further, the deposition rate plateaus, indicating the kinetics transitions to a mass transfer regime where the deposition rates are less dependent on the filament temperature.[14] Polymerization of the CHMA films using TBPO as the initiator could be achieved with filament temperatures >250 °C, whereas TBPOB permits deposition at filament temperature as low as 150 °C. Furthermore, in the mass transfer regime, the maximum deposition initiated by TBPOB is approximately twice that observed with ones initiated by TBPO. Holding all other conditions fixed, reactions initiated by TBPOB have a faster deposition rate than reactions initiated by TBPO. The TBPOB decomposes into both t-butoxy and benzoate radicals, where the latter is much less volatile. Therefore, we hypothesize that the benzoate radicals have a higher surface concentration and thus have a higher probability of reacting with the monomer and result in a faster growth rate. The faster deposition rates are important in situations where thick films are required. High rates also improve the economics of the iCVD process. The ability to initiate polymerizations at a much lower filament temperature reduces heat load to substrate.[32] Thus,

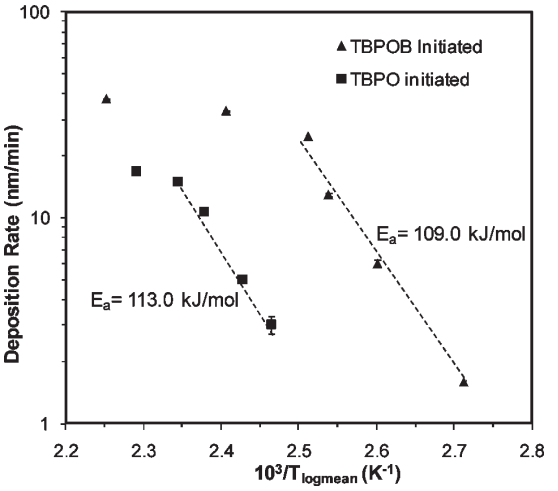

Figure 3. Deposition rate (logarithmic scale) as a function of inverse logarithmic mean of the filament and substrate temperature. Apparent activation energies of 113.0 ± 5.3 and 109.0 ± 4.5 kJ/mol are calculated for TBPO- and TBPOB-initiated reactions.

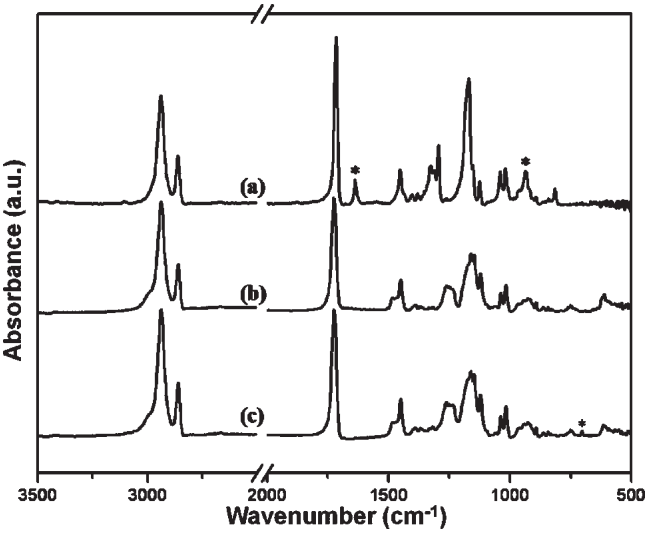

Figure 4. Fourier transform IR (FTIR) spectra of (a) cyclohexyl methacrylate (CHMA) monomer, (b) iCVD poly(cyclohexyl methacrylate) (pCHMA) using TBPO as an initiator, and (c) iCVD deposited pCHMA using TBPOB as an initiator. Asterisks (*) represent signature vinyl bonds in (a), and the out-of-plane C−H bending vibrations for benzene derivatives at 700 cm^{-1} in (c).

TBPOB has the great potential for situations where temperature-sensitive substrates are used. It is also superior to TBPO when using monomer precursors that decompose at high temperatures, thus expanding the applicability of iCVD to new types of polymers.

For solution synthesis using cumene as the solvent, TBPO has a higher reported activation energy (153.46 kJ/mol) than TBPOB (134 kJ/mol).[33] Although solution synthesis takes place at a single uniform temperature, in iCVD there is a temperature gradient between the filament and the substrate. For TBPO, this apparent difficulty was previously resolved by Ozaydin-Ince by employing the logarithmic mean of T_f and T_s in the Arrhenius analysis.[14] Thus, Figure 3 shows the logarithmic of the deposition

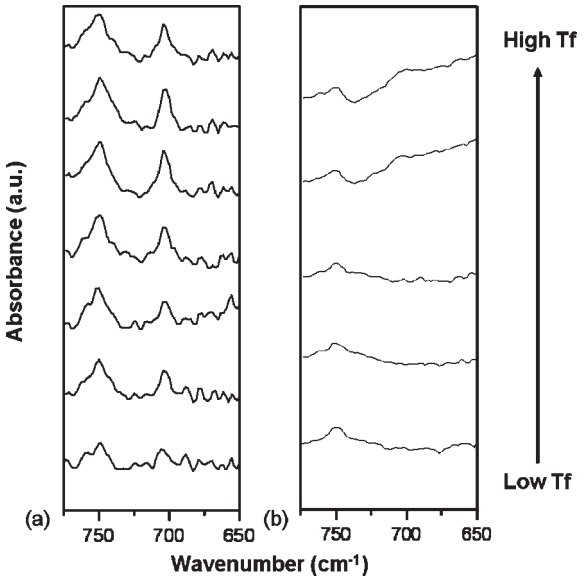

Figure 5. Fourier transform IR (FTIR) spectra of (a) iCVD deposited poly(cyclohexyl methacrylate) (pCHMA) using TBPOB as an initiator at filament temperatures of 150, 206, 228, 238, 257, 280, and 350 °C, and (b) iCVD deposited pCHMA using TBPO as an initiator at filament temperatures of 257, 271, 292, 307, and 331 °C.

Table 1. Atomic Percentages from XPS Survey Scan

	theoretical atomic %	experimental atomic % (TBPO initiated)	experimental atomic % (TBPOB initiated)
carbon	83.33	83.63	83.87
oxygen	16.67	16.37	16.13

rate as a function of the inverse logarithmic mean of T_f and T_s, resulted in estimated apparent activation energies of 113.0 ± 5.3 kJ/mol and 109 ± 4.5 kJ/mol for TBPO- and TBPOB-initiated reactions, respectively. These values are below that of the cleavage of the O−O bond in the initiators. Previously, such lower values have indicated the presence of loading effect, which was alleviated by increasing the monomer flow rate to limit the degree of reactant utilization.[14]

Confirmation of Polymerization by FTIR. Figure 4 shows the FTIR spectra of CHMA monomer precursor, the iCVD deposited pCHMA films using TBPO and TBPOB as the initiators. Successful vinyl polymerization is confirmed by the reduction of unsaturated carbon peaks, as denoted by asterisks in Figure 4a. Most clearly resolved is the sharp C═C stretching mode at 1630 cm^{-1}, the CH_2 wag in vinylidine ($R_2C═CH_2$) at 900 cm^{-1} and the α,β-unsaturated ester (C═C−CO−O−C) stretching at 1300 cm^{-1}. The spectra for both types of iCVD films (Figures 4b and 4c) contain peaks that are characteristic of CHMA: the CH_2 antisymmetrical and symmetrical cyclohexyl vibrations (2939.2 and 2861.4 cm^{-1}), C═O stretching (centered at 1714.6 cm^{-1}), C−H bending (1500−1350 cm^{-1}), and (O═)C−O stretching (1300−1150 cm^{-1}). The high incorporation of pendant cyclohexyl rings from the monomer indicates that iCVD is a non-destructive process and is able to retain the functionality.

As seen by comparing spectra b and c in Figure 4, the majority of the peak locations and areas of the TBPOB initiated polymer spectrum match well with the TBPO initiated one. However,

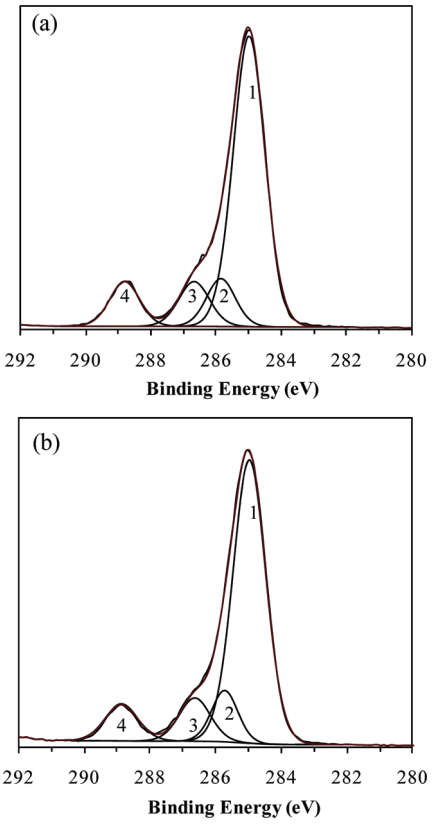

Figure 6. Least-squares regressions of the high-resolution scans of C1s using components with Gaussian lineshapes of pCHMA samples initiated by (a) TBPO and (b) TBPOB. Flow rates of CHMA monomer, TBPO and TBPOB initiators are 4.6, 0.6, and 0.6 sccm. The substrate temperature is 30 °C, filament temperature is 257 °C, and monomer partial pressure ratio is 0.45 for both sets of experiments.

there is a small absorption peak at ∼700 cm^{-1} observed only in Figure 4c, which confirms incorporation of TBPOB into the polymer chain. Indeed, most of monosubstituted benzenes absorb at 697 ± 11 cm^{-1}, which is due to out-of-plane ring bending by sextants. A closer look of this region is shown in Figure 5. Clearly, TBPO-initiated films lack absorption at ∼700 cm^{-1} but for TBPOB initiated films, the peaks are observed in each film and their intensity increases with increasing filament temperature. At higher filament temperature, more initiator radicals are formed and permit higher degree of end group incorporation. The ability to detect aromatic end groups via FTIR is an advantage of the TBPOB initiator. In contrast, the aliphatic chain ends produced using TBPO do not produce easily resolvable FTIR signatures.

Compositional Analysis by XPS. Table 1 shows the atomic concentration percentages calculated from the XPS survey scans. Excellent agreement is observed between the experimentally obtained percentages and the theoretical values calculated from the chemical formula of the monomer. Figure 6 shows the carbon C 1s high-resolution XPS scans for both TBPO and TBPOB initiated pCHMA polymer films. The spectra can be described using four bonding environment expected solely due to vinyl polymerization of the monomer (Table 2). Again, the agreement of both the binding energies and peak area ratios of iCVD films with the theoretical values shows that the structure of the monomer unit is completely maintained during the iCVD

Table 2. High-Resolution C 1s Peak Fit Results for pCHMA

	theoretical[34]		experimental (TBPO initiated)		experimental (TBPOB initiated)	
	binding energy (eV)	area (%)	binding energy (eV)	area (%)	binding energy (eV)	area (%)
1 −C−C*H_2−C−	285.0	70.0	285.0	69.2	285.0	70.3
2 −C*H−CO−O−	285.7	10.0	285.8	10.4	285.7	10.3
3 −CH_2−C*H−O−	286.6	10.0	286.7	10.4	286.6	10.3
4 −O−C*═O	288.9	10.0	288.8	10.0	288.9	9.0

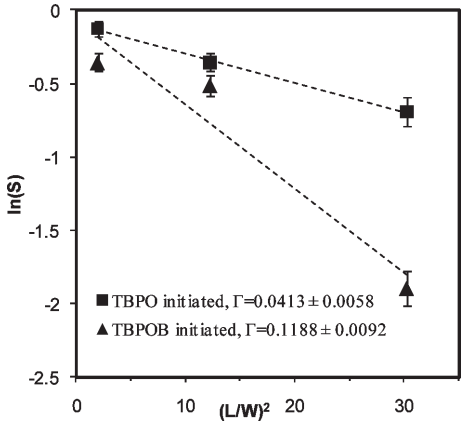

Figure 7. Step coverage as a function of aspect ratio square. The dashed lines represent the linear best-fit lines for the data and the slopes are proportional to the sticking probability of the initiating radicals. Here the three different aspect ratios for the trenches are 5.5, 3.4, and 1.4, respectively. Flow rates of CHMA monomer, TBPO and TBPOB initiators are 4.6, 0.6, and 0.6 sccm. The substrate temperature is 30 °C, filament temperature is 257 °C, and monomer partial pressure ratio is 0.45 for both sets of experiments.

polymerization.[34] The XPS spectra (Figure 6, Table 1, Table 2) of the films initiated by TBPOB and TBPO are similar, indicating that the initiator does not change the chemical composition in the film. However due to the low percentage of initiator incorporated into the polymer films, the benzyl peaks from the TBPOB cannot be resolved in the XPS spectra.

Both FTIR and XPS data support the hypothesis that iCVD produces linear polymeric structure and retains essentially all the pendant cyclohexyl ring functional groups. We expect that TBPOB can be used to initiate iCVD from most, if not all, of the monomers that deposit under TBPO initiation. TBPOB initiated polymer films have similar FTIR and XPS spectrum as TBPO initiated films and show a signature benzene adsorption peak in FTIR. This is the first time that TBPOB has successfully been used in the iCVD system. It not only broadens the iCVD initiator library, but also enables a faster deposition rate and the applications where temperature sensitive substrates and monomers are desired.

Conformality Analysis by SEM. For applications including microfluidics, medical devices, and membranes, good step coverage over nonplanar or porous substrates is desired. Step coverage is defined as the ratio of the coating thickness at the bottom to that at the top of the trench. Figure 7 shows the step coverage for TBPO and TBPOB initiated iCVD pCHMA films on trenches with different aspect ratios. All the experimental conditions including filament temperature, flow rates of initiator and monomer precursors, and substrate temperature were held same between the two experiments. The dashed line shows the linear best-fit between logarithm of step coverage and the square of the aspect ratio. For TBPO initiated depositions, the radical sticking coefficient, Γ_{TBPO}, is found from the slope as 0.0413 ± 0.0058, at P_m/P_{sat} of 0.45 and $T_{filament}$ of 257 °C. This value agrees well with Baxamusa's results for the same polymer at a similar P_m/P_{sat}.[13] Performing a similar analysis for the data of TBPOB initiated depositions, a sticking coefficient value of 0.1188 ± 0.0092 is obtained, which is ∼ three times as high as Γ_{TBPO}. Because the pCHMA is the identical precursor, the difference in conformality between TBPO- and TBPOB-initiated depositions confirms the earlier hypothesis[13] that the sticking probability of the initiator radical controls the observed conformality.

Cross-sectional SEM micrographs (Figure 8a,b) demonstrate the overall profiles for polymer films growing inside trenches with the aspect ratio of 1.4 by iCVD. Both of them show good thickness uniformity over the entire trench feature, however, the conformality of the TBPO initiated iCVD film is superior to that of TBPOB initiated layer, which is due to its lower sticking coefficient. The thermal decomposition of TBPOB results in the production of both *tert*-butoxy and oxybenzoate radicals, which can then adsorb on the substrate surface. *tert*-Butoxy radicals have a higher probability to desorb back into the vapor phase and benzoate radicals are more likely to react with a monomer to form a polymer chain. With lighter *tert*-butoxy radicals continuing down the trench to initiate polymerization, TBPO-initiated films are expected to have a better conformality than TBPOB-initiated films.

The dependence of the step coverage on the radical concentration is studied by varying the filament temperature while keeping the monomer surface concentration constant. Substrate cooling can be made difficult by the insulating nature of the vacuum environment and when substrates of low conductivity are used, such as polymers, textiles, and porous materials. More traditional substrates like silicon and metal have higher thermal conductivity and more readily spread heat to counteract the development of temperature gradients. It has been previously found that substrate temperature (T_s) is a function of the chiller temperature (T_c) and filament temperature because of this imperfect heating.[32] The substrate temperature in this study was kept constant by adjusting T_c at different filament temperatures using the equation:[32] $T_s = 0.88T_c + 0.04T_f + 0.4006$.

As the filament temperature increases, the concentration of the free radicals, formed by thermal dissociation of the initiator, increases as well. Figure 8c shows the effect of filament temperature on the step coverage of trenches with the aspect ratio of 1.4 and $P_m/P_{sat} = 0.45$. In this work, the Thiele modulus ≪1 for both TBPO- and TBPOB-initiated depositions, indicating that the diffusion is fast enough to prevent the build-up of gas phase concentration gradients of the monomer and therefore the conformality is only determined by sticking probability of the

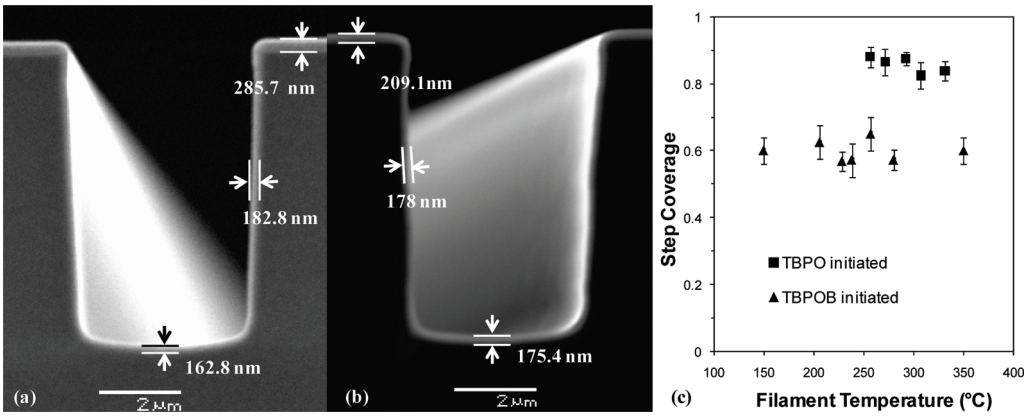

Figure 8. Cross-sectional SEM images of (a) iCVD deposited poly(cyclohexyl methacrylate) (pCHMA) using TBPOB as an initiator, (b) iCVD deposited pCHMA using TBPO as an initiator, and (c) the step coverage as a function of filament temperature. The error bar represents the uncertainty in the measurement of step coverage. Flow rates of CHMA monomer, TBPO, and TBPOB initiators are 4.6, 0.6, and 0.6 sccm. The substrate temperature is 30 °C and monomer partial pressure ratio is 0.45 for both sets of experiments.

initiator. Independence of the step coverage from the filament temperature when using either initiator shows that the radical concentration does not affect the sticking coefficients of the initiating radicals. The results agree well with previous study on the effect of radical initiator concentration on step coverage by varying the initiator flow rates.[35] The data further confirms that TBPO-initiated films exhibit a better conformality than TBPOB-initiated ones at all different filament temperatures when the monomer surface concentration is fixed.

CONCLUSIONS

We have successfully delivered TBPOB into the reactor and used it as an initiator in the iCVD system for the first time. It permitted the TBPOB-initiated thin film deposition to occur at ~80 °C lower than TBPO, at a similar deposition rate. Low filament temperature is advantageous for polymeric substrates which are temperature sensitive or have low glass transition temperatures and additionally for monomers that decompose at high temperatures. It also reduces the cost of the process because less energy is needed, and therefore it is beneficial for an industrial application. Under the exactly same experimental conditions and a filament temperature of 270 °C, TBPOB-initiated polymerization has a deposition rate 7 times higher than TBPO-initiated polymerization, which makes TBPOB a desired choice where high deposition rates are required.

FTIR and XPS results showed the similarity of the chain structure of TBPOB- to the TBPO-initiated films. The only detectable difference is in end groups with the aromatic group in TBPOB providing a unique spectral signature in the FTIR. This peak intensity increased with increase in filament temperature, corresponding to a decrease in number average molecular weight of the TBPOB-initiated pCHMA.

The conformality achieved in the trenches is governed by their aspect ratio and the sticking coefficient of the initiators. The larger oxybenzyl radical produced thus has a higher sticking coefficient than the t-butoxy, which resulted in slightly lower step coverage of TBPOB versus TBPO initiated iCVD pCHMA films over non-planar structures. A higher filament temperature provided a higher initiator radical concentrations and more FTIR-observable end groups in the layers grown using TBPOB. At constant surface monomer concentration, increasing the concentration of initiator radicals does not affect the step coverage of the trenches, which indicates that surface monomer concentration is the species determining step coverage.

AUTHOR INFORMATION

Corresponding Author

*Corresponding author email: kkg@mit.edu.

ACKNOWLEDGMENT

The authors acknowledge financial support of the MIT Institute for Soldier Nanotechnologies (ISN) under Contract DAAD-19-02D-0002 with the U.S. Army Research Office. We thank Dr. Elisabeth Shaw from MIT Center for Materials Science and Engineering (CMSE) for her assistance with XPS measurements. Dr. Edward F. Gleason of Analog Devices is thanked for supplying the trench wafer substrates. We are also grateful for the helpful discussions that Dr. Gozde Ozaydin-Ince, Dr. Salmaan Baxamusa, and Dr. Wyatt Tenhaeff provided.

REFERENCES

(1) Wilson, J. T.; Cui, W. X.; Chaikof, E. L. *Nano Lett.* **2008**, *8*, 1940–1948.
(2) Stoldt, C. R.; Carraro, C.; Ashurst, W. R.; Gao, D.; Howe, R. T.; Maboudian, R. *Sens. Actuators, A* **2002**, *97-98*, 410–415.
(3) Asatekin, A.; Gleason, K. K. *Nano Lett.* **2011**, *11*, 677–686.
(4) Ozaydin-Ince, G.; Dubach, J. M.; Gleason, K. K.; Clark, H. A. *Proc. Natl. Acad. Sci. U.S.A.* **2011**, *108*, 2656–2661.
(5) Elam, J. W.; Routkevitch, D.; Mardilovich, P. P.; George, S. M. *Chem. Mater.* **2003**, *15*, 3507–3517.
(6) Alf, M. E.; Asatekin, A.; Barr, M. C.; Baxamusa, S. H.; Chelawat, H.; Ozaydin-Ince, G.; Petruczok, C. D.; Sreenivasan, R.; Tenhaeff, W. E.; Trujillo, N. J.; Vaddiraju, S.; Xu, J. J.; Gleason, K. K. *Adv. Mater.* **2010**, *22*, 1993–2027.
(7) Dameron, A. A.; Seghete, D.; Burton, B. B.; Davidson, S. D.; Cavanagh, A. S.; Bertrand, J. A.; George, S. M. *Chem. Mater.* **2008**, *20*, 3315–3326.
(8) Chen, Y.; Haddon, R. C.; Fang, S.; Rao, A. M.; Lee, W. H.; Dickey, E. C.; Grulke, E. A.; Pendergrass, J. C.; Chavan, A.; Haley, B. E.; Smalley, R. E. *J. Mater. Res.* **1998**, *13*, 2423–2431.
(9) Kim, J. H.; Park, P. K.; Lee, C. H.; Kwon, H. H. *J. Membr. Sci.* **2008**, *321*, 190–198.
(10) Xu, J. J.; Gleason, K. K. *Chem. Mater.* **2010**, *22*, 1732–1738.

(11) Tenhaeff, W. E.; McIntosh, L. D.; Gleason, K. K. *Adv. Funct. Mater.* **2010**, *20*, 1144–1151.
(12) Yang, R.; Xu, J. J.; Ozaydin-Ince, G.; Wong, S. Y.; Gleason, K. K. *Chem. Mater.* **2011**, *23*, 1263–1272.
(13) Baxamusa, S. H.; Gleason, K. K. *Chem. Vap. Deposition* **2008**, *14*, 313–318.
(14) Ozaydin-Ince, G.; Gleason, K. K. *J. Vac. Sci. Technol., A* **2009**, *27*, 1135–1143.
(15) Lau, K. K. S.; Gleason, K. K. *Adv. Mater.* **2006**, *18*, 1972–1977.
(16) Im, S. G.; Bong, K. W.; Kim, B. S.; Baxamusa, S. H.; Hammond, P. T.; Doyle, P. S.; Gleason, K. K. *J. Am. Chem. Soc.* **2008**, *130*, 14424.
(17) Denisova, E. T.; Denisova, T. G.; Pokidova, T. S. *Handbook of Free Radical Initiators*; Wiley: New York, 2003.
(18) Yasutake, M.; Hiki, S.; Andou, Y.; Nishida, H.; Endo, T. *Macromolecules* **2003**, *36*, 5974–5981.
(19) Lau, K. K. S.; Gleason, K. K. *Macromolecules* **2006**, *39*, 3688–3694.
(20) Kramer, N. J.; Sachteleben, E.; Ozaydin-Ince, G.; van de Sanden, R.; Gleason, K. K. *Macromolecules* **2010**, *43*, 8344–8347.
(21) Tenhaeff, W. E.; McIntosh, L. D.; Gleason, K. K. *Adv. Funct. Mater.* **2010**, *20*, 1144–1151.
(22) Trujillo, N. J.; Wu, Q. G.; Gleason, K. K. *Adv. Funct. Mater.* **2010**, *20*, 607–616.
(23) Martin, T. P.; Kooi, S. E.; Chang, S. H.; Sedransk, K. L.; Gleason, K. K. *Biomaterials* **2007**, *28*, 909–915.
(24) Lewis, H. G. P.; Caulfield, J. A.; Gleason, K. K. *Langmuir* **2001**, *17*, 7652–7655.
(25) Chan, K.; Gleason, K. K. *Chem. Vap. Deposition* **2005**, *11*, 437–443.
(26) Chan, K.; Gleason, K. K. *Langmuir* **2005**, *21*, 11773–11779.
(27) O'Shaughnessy, W. S.; Baxamusa, S.; Gleason, K. K. *Chem. Mater.* **2007**, *19*, 5836–5838.
(28) Nozaki, K.; Bartlett, P. D. *J. Am. Chem. Soc.* **1946**, *68*, 1686–1692.
(29) Nakata, T.; Tokumaru, K.; Simamura, O. *Tetrahedron Lett.* **1967**, 3303.
(30) Sacak, M.; Oflaz, F. *J. Appl. Polym. Sci.* **1993**, *50*, 1909–1916.
(31) Cheng, S. Y.; Tseng, J. M.; Lin, S. Y.; Gupta, J. P.; Shu, C. M. *J. Therm. Anal. Calorim.* **2008**, *93*, 121–126.
(32) Gupta, M.; Gleason, K. K. *Thin Solid Films* **2006**, *515*, 1579–1584.
(33) *Polymer Handbook*, 4th ed.; Brandrup, J., Immergut, E. H., Grulke, E. A., Eds.; Wiley-Interscience: New York, 1999.
(34) Beamson, G.; Briggs, D. *High Resolution XPS of Organic Polymers: The Scienta ESCA300 Database*; John Wiley & Sons: Chichester, UK, 1992.
(35) Ozaydin-Ince, G.; Gleason, K. K. *Chem. Vap. Deposition* **2010**, *16*, 100–105.